

AN EXPERIMENTAL COMPARISON OF SINGLE CRYSTAL CVD DIAMOND AND 4H-SiC SYNCHROTRON X-RAY BEAM DIAGNOSTICS

C. Houghton*, C. Bloomer, L. Bobb, Diamond Light Source, OX11 0DE, Didcot, United Kingdom

Abstract

As synchrotron beamlines increasingly use micro-focus techniques with detectors sampling at kHz rates, the need for real-time monitoring of the beam position at similar bandwidths is vital. Commercially available single-crystal CVD diamond X-ray diagnostics are well established as excellent non-destructive monitors for synchrotron X-ray beamlines. Silicon carbide (4H-SiC) X-ray beam position monitors (XBPMs) are a recent development with the potential to provide the same benefits as their diamond counterparts with larger usable apertures and lower cost. At Diamond Light Source a comparison between single-crystal CVD diamond and 4H-SiC XBPMs has been carried out. The sc-diamond and 4H-SiC beam position monitors are mounted in-line along the beam path, so that synchronous kHz measurements of the synchrotron X-ray beam motion can be measured. Several tests of the two position monitors performance are presented: comparing kHz beam position measurements from the detectors, temporal response, and signal uniformity across the face of the detectors. Each test is performed with varying bias voltages applied to the detectors. A discussion of the benefits and limitations of 4H-SiC and diamond detectors is included.

INTRODUCTION

With the recent upgrades to synchrotron beamline optics that allow for sub-micron X-ray beam sizes at the sample point, and beamline detectors with operating frequencies in the kHz range, the need for accurate beam position monitoring at similar bandwidths is essential. Destructive X-ray beam position diagnostics such as fluorescent screens can not be used during experimental data collection as the transmission of X-rays through the materials used for these screens is low. For example 50 μm of LuAG scintillator has a transmission of just 7% at 9 keV [1]. Modern beamlines require real-time non-destructive beam position monitoring to ensure the micro-focus beam is stable throughout any data collection. This demand led to the research and development of diamond X-ray Beam Position Monitors (XBPMs) due to their excellent transparency, radiation hardness, and thermal conductivity.

Early experiments with polycrystalline diamond [2,3] have led to modern, commercially available single-crystal chemical vapour deposition (scCVD) diamond XBPMs with beam position resolutions of a few 10 nm [4]. These XBPMs perform as excellent non-destructive monitors for synchrotron X-ray beamlines.

Silicon carbide (4H-SiC)¹ XBPMs are a more recent development that have the potential to provide the same benefits as their diamond counterparts with the added benefit of larger usable apertures and potentially lower cost [5]. In this paper a direct comparison of these two devices is conducted on a synchrotron X-ray beamline.

EXPERIMENTAL SET-UP

The experiment was conducted on the I18 [6] beamline at Diamond Light Source. The two XBPMs used in this experiment were a 10.5 μm thick 4H-SiC detector and a 50 μm thick single-crystal CVD diamond, referred to as sc-diamond. The thicknesses of these devices were chosen such that the two detector plates have similar X-ray transmission at typical synchrotron beamline photon energies. For example, the following experiments were conducted at 9 keV, where transmission is 95% and 90% for the sc-diamond and 4H-SiC XBPM respectively [1].

As shown in Fig. 1, the 4H-SiC detector was mounted in front of the sc-diamond as the sc-diamond XBPM has a smaller transparent aperture. These were placed in a nitro-

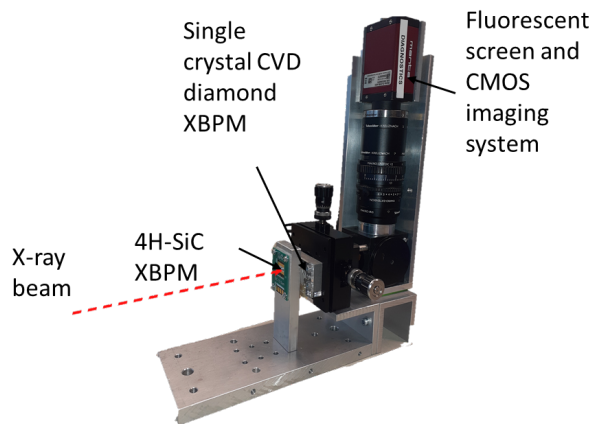


Figure 1: Image of the mounting stage used for the direct comparison of a 4H-SiC XBPM with a sc-diamond XBPM, complete with a CMOS camera imaging system.

gen environment. Behind both the XBPMs was a fluorescent screen CMOS imaging system, used to capture beam images at 700 Hz for independent verification of beam motion. The three devices were secured to a X-Y motion stage just upstream of the sample point, allowing for the X-ray beam to be moved across the surface of the XBPMs. The applied bias voltages and the flux, by use of filters, could be changed throughout the experiment. Generally a 25 μm Al filter was

* claire.houghton@diamond.ac.uk

¹ 4H-SiC refers to the polytype of silicon carbide

Content from this work may be used under the terms of the CC BY 3.0 licence (© 2021). Any distribution of this work must maintain attribution to the author(s), title of the work, publisher, and DOI

in place and the applied bias voltages were 10 V and 5 V for the sc-diamond and 4H-SiC XBPMs respectively.

RESULTS

Signal Uniformity

The motion stage upon which the XBPM and imaging system were mounted could be accurately positioned to within $2\ \mu\text{m}$. This allowed for two-dimensional raster scans to be completed. Figures 2 and 3 show the signal currents obtained during these scans.

One of the main benefits of using 4H-SiC for X-ray beam position measurements is the possibility for larger active regions, meaning larger beam size beamlines can have accurate position data in situ given that larger X-ray beams can be transmitted through the detector. This is demonstrated clearly in Fig. 2, where a $4.5\ \text{mm} \times 4.5\ \text{mm}$ 2-dimensional scan was completed. The signal current generated from each quadrant is shown as a function of the position of the motion stage. The sc-diamond active region is $3\ \text{mm} \times 3\ \text{mm}$ square whereas for 4H-SiC this region is $9\ \text{mm} \times 3\ \text{mm}$. Both de-

vices show good signal uniformity across the surface. In Fig. 2 the 4H-SiC's four rectangular quadrants are visible, along with a strip of surface metallisation extending from each. This strip is used to carry the signal currents closer to the edge of the SiC plate, to reduce the need for long a delicate wire bonds.

The uniformity of the signal across both devices is further demonstrated in Fig. 3 where a finer detail $0.17\ \text{mm} \times 0.17\ \text{mm}$ raster scan was completed. The current measured by the first quadrant (A) for both devices is shown. Visually the signal uniformity of two devices is indistinguishable.

Temporal Response

An experiment to determine the resolution limitations and the temporal response of the detectors was carried out. The aim of this measurement was to determine whether the beam motion measured on both of the XBPMs when the beam is centred on the quadrants is 'real' beam motion rather than intrinsic noise from the detector or acquisition electronics. To verify the beam motion a fluorescent screen CMOS imaging system was used. The images from the CMOS camera were

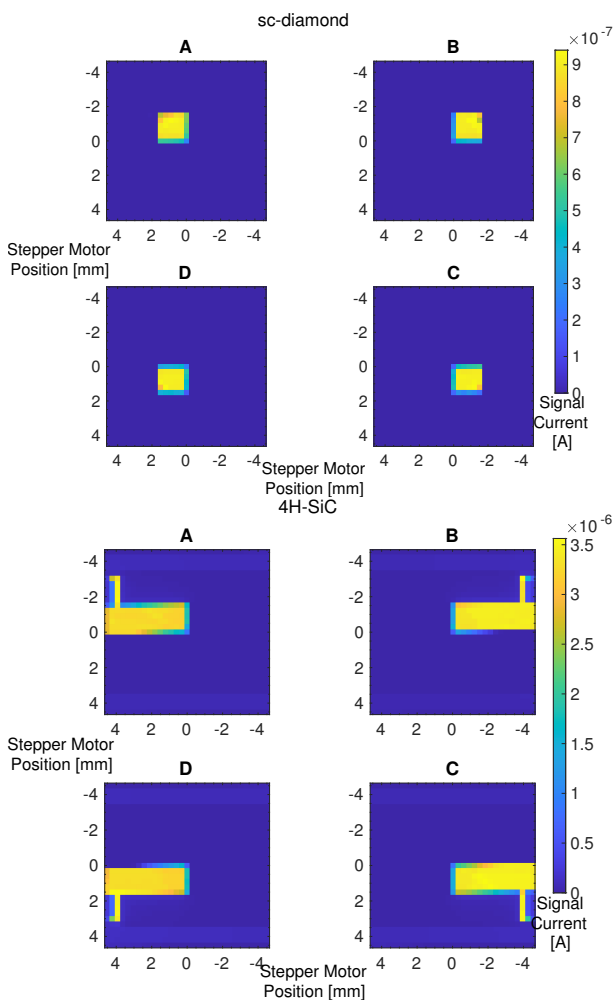


Figure 2: Two-dimensional $4.5\ \text{mm}$ raster scan across the surface of (top) a $50\ \mu\text{m}$ thick sc-diamond XBPM, and (bottom) a $10.5\ \mu\text{m}$ thick 4H-SiC XBPMs.

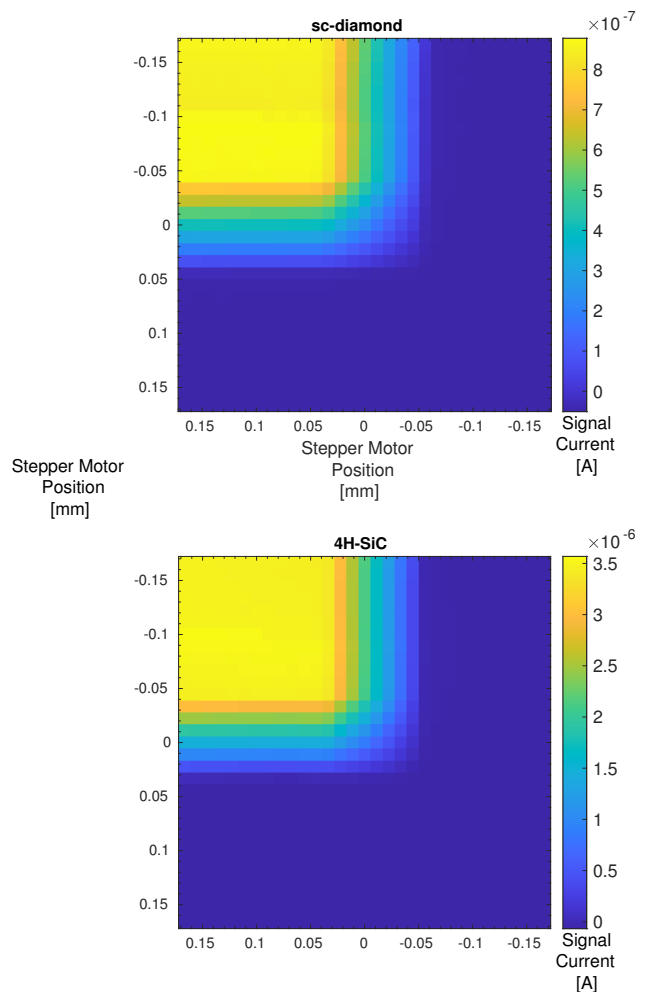


Figure 3: Two-dimensional $0.17\ \text{mm}$ raster scan across a single quadrant (A) of the surface of (Top) $10.5\ \mu\text{m}$ thick 4H-SiC XBPM and (Bottom) $50\ \mu\text{m}$ thick sc-diamond XBPMs.

analysed using a 2D Gaussian fit to provide independent beam position measurements. The frame rate of the camera was 700 Hz, much lower than the 20 kHz data collected by the XBPMs. However, it is still a good benchmark to corroborate the beam movement.

Presented in Fig. 4 are the intensity measurements for both the sc-diamond XBPM and 4H-SiC XBPM over 200 ms. The beam intensity measured from the sum of all pixels from the CMOS camera data has been plotted with the XBPM intensity measurement. The data has been normalised to the mean intensity for each device, and shows clear correlation. Therefore the 4H-SiC XBPM can work as a good non-destructive intensity monitor on beamlines, equally as responsive on ~ 10 ms timescales as a traditional sc-diamond XBPM.

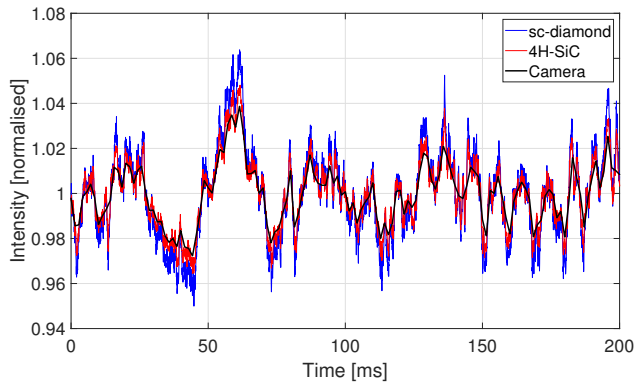


Figure 4: The X-ray beam intensity synchronously recorded by a sc-diamond and 4H-SiC XBPMs at 20 kHz. Intensity is calculated by the summing of all four XBPM quadrants. Also shown, as an independent measurement of intensity from a CMOS camera running at 700 Hz.

In addition, the position measurements for both XBPM devices are plotted in Fig. 5. The horizontal and vertical beam positions, x and y respectively can be determined from the XBPM 4 quadrant signals, Equation (1)

$$x = K_x \frac{(I_A + I_D) - (I_C + I_B)}{I_A + I_B + I_C + I_D} \quad (1a)$$

$$y = K_y \frac{(I_A + I_B) - (I_C + I_D)}{I_A + I_B + I_C + I_D} \quad (1b)$$

where $I_{(A,B,C,D)}$ are the currents through the four XBPM quadrants (A = top-left; B = top-right; C = bottom-right; D = bottom-left), and K_x and K_y are the scale factors for horizontal and vertical respectively.

Figure 5 shows vertical beam position over 200 ms for the 4H-SiC, sc-diamond XBPMs, and the camera. With a scale factor K_y of 100 μm and 50 μm for 4H-SiC and sc-diamond respectively. A 2D Gaussian fit was applied to the camera images where the calculated centroid is taken as the beam position. The small intrinsic beam motion present at the sample point due to the monochromator, slits and other optical elements can be seen on all of the devices. It is clear the camera does not have the temporal resolution to pick

up some of the motion of the beam which both the XBPMs can measure. However, the two XBPM measurements show good agreement.

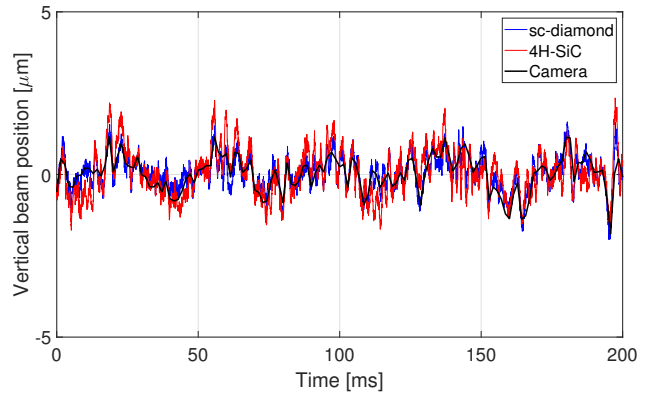


Figure 5: The vertical beam position synchronously recorded by a sc-diamond and 4H-SiC XBPMs at 20 kHz. Also shown, as an independent measurement of beam position from a CMOS camera running at 700 Hz.

Flux Linearity

Both sc-diamond and 4H-SiC detector materials use the same fundamental detection mechanism, where absorbed ionizing radiation excites electrons from the atomic valance band into the conduction band. The resulting signal current is proportional to the number of charge carriers that are excited, and proportional to the energy absorbed within the detector material. For diamond detectors it has been verified that for a given photon energy the signal current is extremely linear with respect to incident flux, over many orders of magnitude [7].

A measure of the flux linearity of the 4H-SiC detector with respect to the diamond XBPM was carried out. The I18 beamline at DLS has the ability to attenuate the incident beam by using various thickness of filter material. Figure 6 shows the resultant plot, with the results for the 4H-SiC XBPM plotted against the sc-diamond producing the expected linear plot. The small discrepancy observed at ~ 1 nA is likely a result of errors in the measuring equipment, rather than differences in signal generation. As it is already well established that sc-diamond XBPMs are linear with incident flux it is possible to conclude that the 4H-SiC XBPM is also linear with flux over the evaluated intensity range.

Bias Requirements

The sensitivity of single-crystal diamond detectors can be influenced by the magnitude of the bias voltage applied across the bulk diamond [7]. With higher voltage more of the charge carriers will be collected at the measurement electrodes, and there is less time for diffusion of the charge carriers leading to a more accurate beam profile measurement [8].

The 4H-SiC detectors are doped so as to operate as a p-n junction diode [5]. The result is an effective ‘built-in’

Content from this work may be used under the terms of the CC BY 3.0 licence (© 2021). Any distribution of this work must maintain attribution to the author(s), title of the work, publisher, and DOI

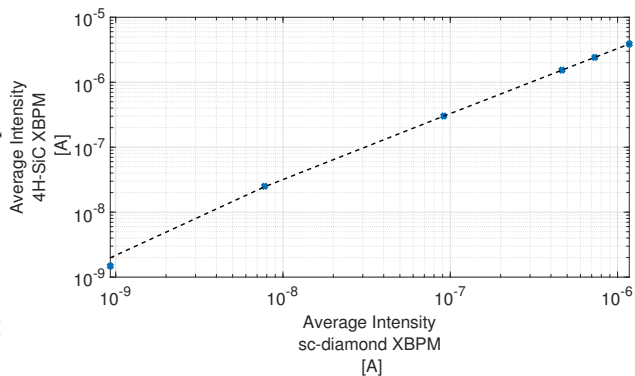


Figure 6: The average intensity of the 4H-SiC XBPM, calculated by summing all 4 quadrants, plotted against the same variable for the sc-diamond XBPM in a log-log plot. Dotted Line: The linear fit of the data points shown as blue dots.

electric field that enables operation of the 4H-SiC device at zero bias voltage. In contrast, due to the difficulty in doping sc-diamond [9, 10], virtually all commercial sc-diamond detectors require an external bias voltage to be supplied.

Figure 7 shows the measured current on two of the quadrants as a one-dimensional stepper motor scan was taken. On the left portion of the scan only quadrant ‘A’ is illuminated, and on the right only quadrant ‘D’ is illuminated. This shows the cross over between the two quadrants, which in both XBPMs is visually symmetrical. As expected the sc-diamond XBPM requires a minimum of 0.5 V in order to achieve something close to full charge collection. However, the 4H-SiC XBPM appears to need no applied bias in order to achieve similar charge collection efficiencies. There is little difference between the currents seen with 0 V and 5 V for the 4H-SiC XBPM, suggesting the detector could be run without the need for a bias voltage supply.

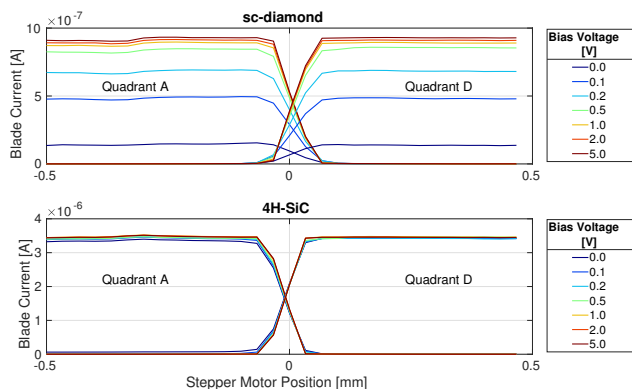


Figure 7: The results of 1D scans of the X-ray beam moving across the face of the detectors, with varying bias voltages applied. Top: 50 μm thick single-crystal diamond. Bottom: 10.5 μm thick 4H-SiC.

Additionally, the beam intensity was calculated as the sum of all the quadrants. An integration period of 1 seconds was used. The charge collection efficiency (CCE) was calculated and is presented in Fig. 8. A charge collection of 100 % is

assumed to have occurred with an applied bias of 5 V. This further confirms the results seen in Fig. 7 the efficiency of the 4H-SiC XBPM does not drop below 90 %, conversely a minimum voltage of 0.5 V is required for the sc-diamond XBPM to reach efficiencies of the same level. Both detectors have the same CCE with bias voltages above 2 V.

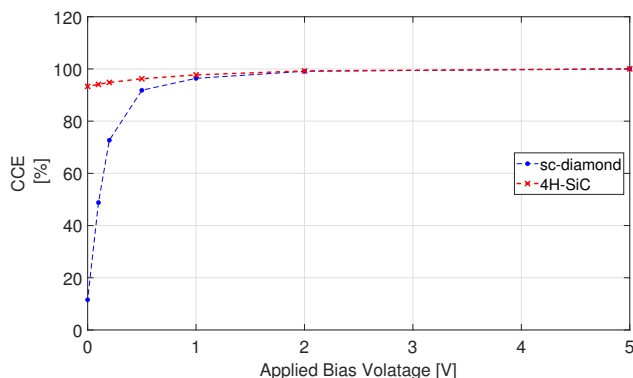


Figure 8: The Charge Carrier Efficiency (CCE) for sc-diamond and 4H-SiC XBPMs with bias voltage, using the average intensity from 30 seconds of 20 kHz data.

CONCLUSION

An experimental comparison between the existing commercially available sc-diamond and a new 4H-SiC non-destructive X-ray beam position monitor has been conducted in a nitrogen environment. The 4H-SiC XBPM has equivalent operational performance to the sc-diamond XBPM in signal uniformity, temporal resolution and flux linearity. 4H-SiC XBPMs can be operated without a bias voltage simplifying the installation on beamlines. In addition, the 4H-SiC can be produced with a larger clear aperture. This is beneficial for beamlines with larger beam sizes where the use of the smaller aperture sc-diamond XBPM would limit performance. Through appropriate choice of 4H-SiC thickness, 4H-SiC detectors can offer comparable transmission to sc-diamond XBPMs for in situ beam position measurements. Based on these results the 4H-SiC should be considered an option for non-destructive monitors for synchrotron X-ray beamlines in the future.

ACKNOWLEDGEMENTS

The authors of this paper would like to thank Konstantin Ignatyev and I18 for the beam time necessary for this experiment. We would also like to thank Cordutza Dragu for the synchronous trigger system used and Graham Cook for his work on the mounting system. Thank you for the support of STLab who provided the 4H-SiC detector for testing.

REFERENCES

- [1] B.L. Henke, E.M. Gullikson, and J.C. Davis, “X-ray interactions: photoabsorption, scattering, transmission, and reflection at E=50-30000 eV, Z=1-92”, *At. Data Nucl. Data Tables*, vol. 54, no. 2, pp. 181-342, July 1993.

- [2] D. Shu, T.M. Kuzay, Y. Fang, J. Barraza, and T. Cundiff, "Synthetic diamond-based position-sensitive photoconductive detector development for the Advanced Photon Source", *J. Synchrotron Rad.*, vol. 5, pp. 636-638, 1998. doi:10.1107/S0909049597019778
- [3] H. Sakae *et al.*, "Diamond Beam-Position Monitor for Undulator Radiation and Tests at the Tristan Super Light Facility", *J. Synchrotron Rad.*, vol. 4, pp. 204-209, July 1997. doi:10.1107/S090904959700561X
- [4] E. Griesmayer, P. Kavargin, C. Weiss, and S. Kalbfleisch, "Applications of single-crystal CVD diamond XBPM detectors with nanometre x-ray beams", *AIP Conference Proceedings*, vol. 2054, pp. 060052, 2019. doi:10.1063/1.5084683
- [5] S. Nida *et al.*, "Silicon carbide X-ray beam position monitors for synchrotron applications", *J. Synchrotron Rad.*, vol. 26, pp. 28-35, 2019. doi:10.1107/S1600577518014248
- [6] JF. Mosselmans *et al.*, "I18—the microfocus spectroscopy beamline at the Diamond Light Source", *J. Synchrotron Rad.*, vol. 16, pp. 818-824, 2009. doi:10.1107/S0909049509032282
- [7] J. Bohon, E. Muller, and J. Smedley, "Development of diamond-based X-ray detection for high-flux beamline diagnostics", *J. Synchrotron Rad.*, vol. 17, pp. 711-718, 2010. doi:10.1107/S0909049510031420
- [8] C. Bloomer and G. Rehm, "The Use of single-crystal CVD diamond X-ray beam diagnostics for synchrotron beamline commissioning and operation at diamond light source Ltd", *2016 IEEE Nuclear Science Symposium, Medical Imaging Conference and Room-Temperature Semiconductor Detector Workshop (NSS/MIC/RTSD)*, pp. 1-7, 2016. doi:10.1109/NSSMIC.2016.8069893
- [9] J. Achard, V. Jacques, and A. Tallaire, "CVD diamond single crystals with NV centres: a review of material synthesis and technology for quantum sensing applications", *J. Phys. D: Appl. Phys.*, vol. 53, pp. 313001, 2020. doi:10.1088/1361-6463/ab81d1
- [10] S. Koizumi, C.E. Nebel, and M. Nesladek, Eds., Weinheim, "Theoretical Models for Doping Diamond for Semiconductor Applications", in *Physics and Applications of CVD Diamond*, Germany: Wiley-VCH Verlag, 2008, pp. 200-236.